inter.noise
HAMBURG 2016

Experimental study on the influence of the sensor and actuator arrangement on the performance of an active noise blocker for a tilted window.

Jonas HANSELKA[1]; Sergej JUKKERT[2]; Delf SACHAU[3]

[1,2,3] Helmut Schmidt University Hamburg, Germany

ABSTRACT

Closed windows reduce noise by approximately 20 dB. Unfortunately, they block fresh air circulation at the same time. To solve this problem, an active noise blocker (ANB) has been set up. It consists of a set of microphones and loudspeakers driven by a MIMO FxLMS (multiple input multiple output filtered reference (x) least mean square) controller on the real time processor. The goal of the ANB is to generate sound pressure nodes to stop the transfer of acoustic energy into the room, using a low but sufficient number of secondary loudspeakers placed in the transmission path. This specific local anti-noise measure shall achieve a high global noise reduction inside the room. Preceding numerical studies have shown, that the arrangement of the sensors and actuators of the ANB in the transmission path has significant effect on its performance. This study checks experimentally different combinations of the setup of the system components with regard to their influence on the performance of the ANB. Additionally this study includes the realization of an add-on kit for an already installed window.

Keywords: Active noise control, broadband, 51.3, 52.2, 52.3, 52.4

1. INTRODUCTION

Active Noise Control (ANC) is a promising attempt to reduce the exposure of city dwellers to excessive traffic noise at home or workplace. Due to increasing road and rail infrastructure the distance between railways and housing sector decreases continuously. Noise barriers, often used as measures against traffic noise, block the view and are not that efficient for low frequencies due to sound diffraction at the upper edge. ANC uses the principle of destructive interference to reduce sound by means of acoustical sensors and actuators (1). The closer the ANC system is installed to the noise source (primary source) inside an enclosed volume, the easier a global noise reduction can be achieved within the volume using a local ANC arrangement (2, 3). The so called ANB reduces significantly the complexity of the system, because it is no more necessary to control the noise within the volume since it is already blocked from entering it.

This paper presents experimental exploration of an ANB which uses a set of 8 actuators (secondary loudspeakers) and 14 sensors (error microphones), controlled by a single reference feed forward filtered x (reference) least mean square algorithm ($1 \times 14 \times 8$ FxLMS) (4) to block the noise directly at the transmission path (tilted window) and calm down the interior space, e.g. a sleeping room. The FxLMS combines an easy implementation with a sufficient robustness to disturbances in the secondary path in that application. Due to the compact system design the possible changes in the secondary paths remain small. Thus, an online update of the secondary paths is unnecessary.

The functionality of this system has already been proven in (3, 5, 6). Here, the different actuator and sensor arrangements are studied to develop a compact ANB system for applications in real environment.

[1] hanselka.jonas@hsu-hh.de
[2] jukkerts@hsu-hh.de
[3] delf.sachau@hsu-hh.de

2. TEST BENCH WITH THE ANB

2.1 Test Bench

For the measurements a transmission test system is used, consisting of an anechoic chamber and a reverberation room connected by an ordinary window. The dimensions in mm of the rooms can be seen in Figure 1. The height of the anechoic chamber is 2500 mm and the height of the reverberation room is 2550 mm. The floor and the ceiling of the anechoic chamber are also covered with noise absorbing wedges, like its walls. The opening in the wall of the reverberation room where the window is placed is 910 mm in width and height and 200 mm in depth. Its lower edge measures 650 mm from the floor.

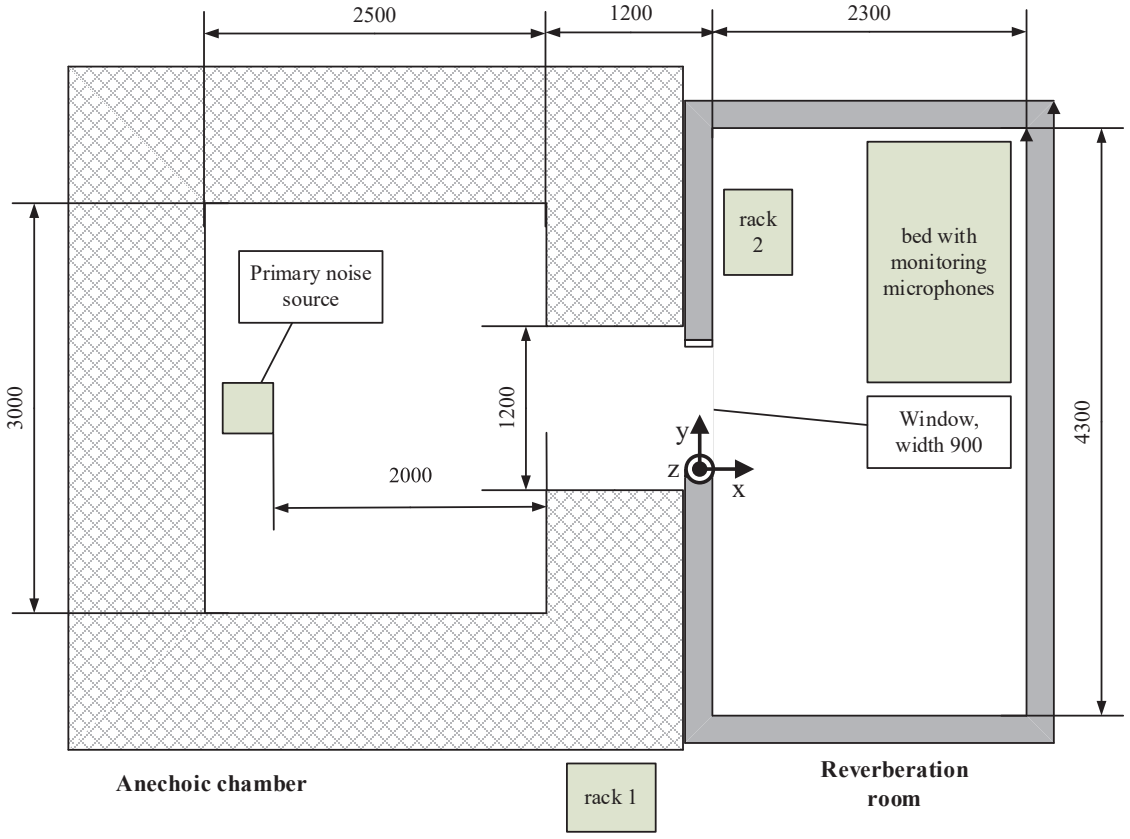

Figure 1 – Ground-plan of the transmission test system (dimensions in mm)

In Figure 2 the setup of the ANB can be seen. The primary noise is emitted by an electro-dynamical loudspeaker (type: Klein + Hummel Pro X12) [2] situated in the anechoic chamber operated by an amplifier (type: PowerSoft Digam LQ2804). The secondary loudspeakers [1] and error microphones [3] (type: Brüel&Kjaer 4958) are arranged around the window [4], the precise configurations are explained in the following section. To monitor the success of the control two monitoring microphones (type: Brüel&Kjaer 2671) are installed in an artificial head [6] inside the reverberation room. A frontend (type: Brüel&Kjaer 3053 B 120) is used for real time data analysis. The controller is executed on a dSpace Rapid Control Prototyping (RCP) processor board DS1006 (AMD Opteron Quad-Core CPU). The anti-aliasing is realized by analog filters (type: SAB S160M) with the corner frequency $f_{\mathrm{c,i}} = 2$ kHz and reconstruction by filters of the same type with $f_{\mathrm{c,o}} = 1$ kHz.

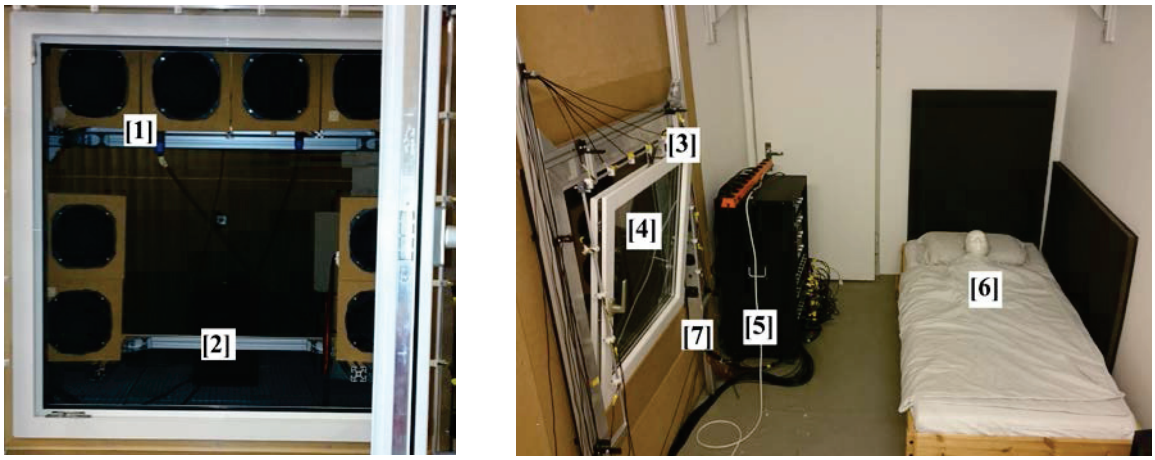

Figure 2 – Experimental setup of the anechoic chamber (left) and the reverberation room (right)

2.2 System Configurations

The appendix contains two tables with the Cartesian coordinates referring to the coordinate system shown in figure 1. The orientations of the perpendiculars of the speakers membranes are listed in the tables too.

The arrangement of the system components for configuration 1 is shown in Figure 3. Secondary loudspeakers with a diameter of $d = 0.16$ m (type: Eighteen sound 6nd430, cabinet dimensions: width 220 mm, height 220 mm, depth 160 mm) are used. The front edge of the cabinets has a distance of 200 mm from the opening in the wall. They are driven by an eight channel amplifier (type: Stageline 1508). The loudspeakers are arranged along the gap of the tilted window inside the anechoic chamber. The distance between the loudspeakers and the error microphones in x-direction is $l = 0.5$ m. The error microphones are installed at a frame along the gap inside the reverberation room, pointing directly into the gap in negative x-direction.

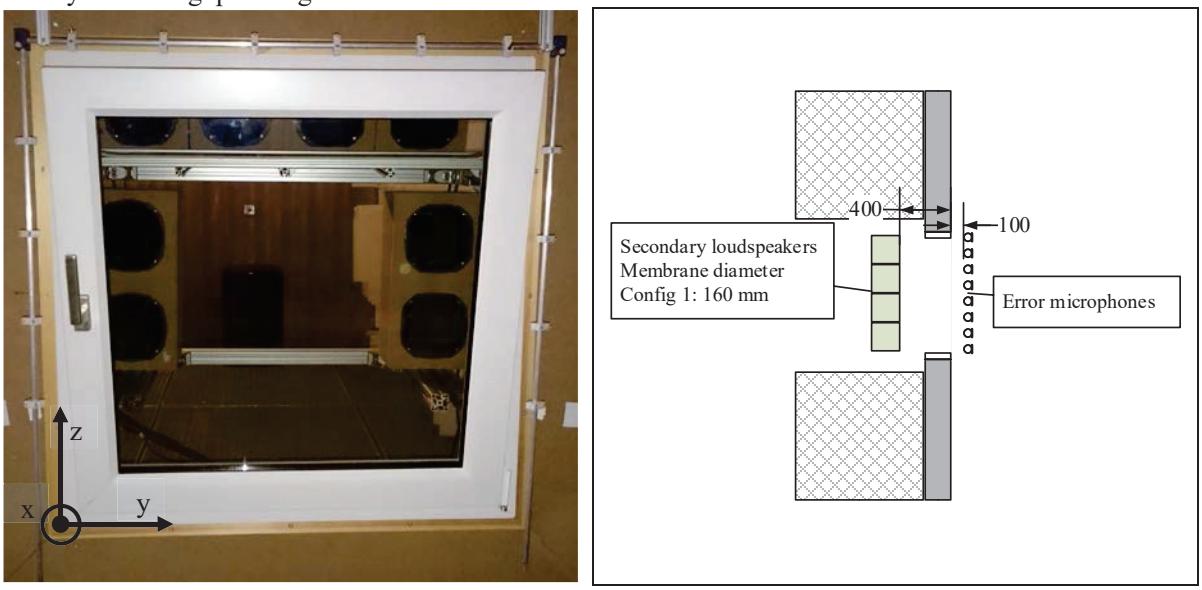

Figure 3 – Setup of configuration 1 front view (left), overview (right)

Configuration 2 uses the same setup with another type of secondary loudspeakers (type: Monacor SH100c, cabinet dimensions: width 160 mm, height 160 mm, depth 320 mm). The speaker membrane amounts $d = 0.08$ m. No further changes are made. The setup is shown in Figure 4.

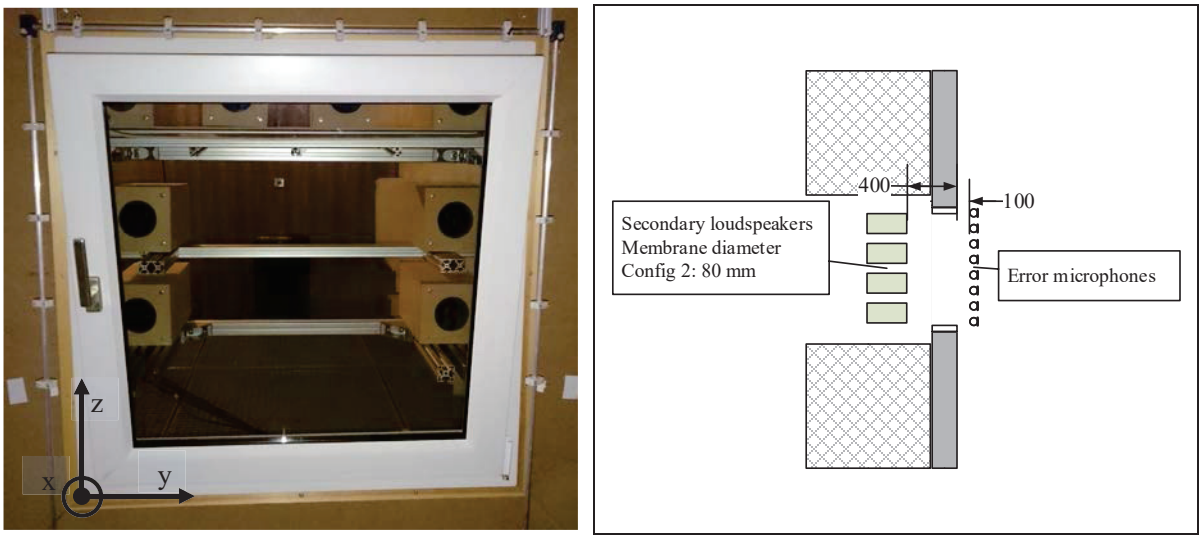

Figure 4 – Setup of configuration 2 front view (left), overview (right)

In configuration 3 the distance between the secondary loudspeakers (same as in configuration 2) and the error microphones is decreased to $l = 0.2$ m by moving the secondary loudspeakers towards the window in positive x-direction. Like this, the front edge of the speakers cabinets reaches 100 mm into the opening in the wall. The cabinets are touching the wall in the opening with their respective right, upper or left side. This means that between the cabinets and the wall no air can pass. The arrangement of the microphones stays unchanged. The setup is shown in Figure 5.

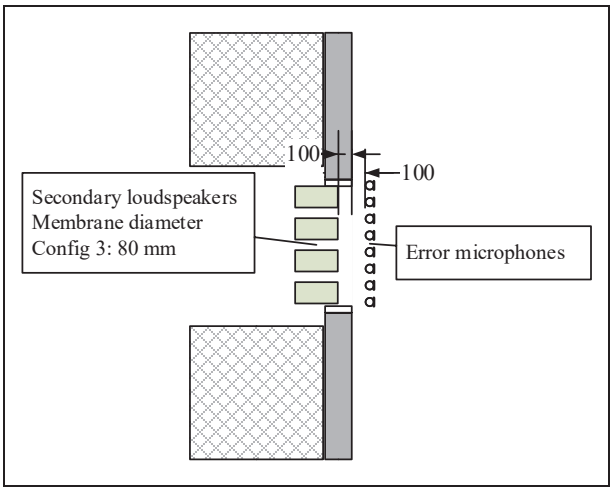

Figure 5 – Setup of configuration 3 overview

In configuration 4 the secondary loudspeakers are erected in the reverberation room with membranes pointing towards the window in negative x-direction. They are slightly rotated around the z-axis. To guarantee that the order of primary source, secondary sources and error microphones regarding the path of sound propagation is maintained, the error microphones are moved towards the reverberation room in positive x-direction. The distance between the cancelling loudspeakers and the error microphones is $l = 0.1$ m. The setup is shown in Figure 6.

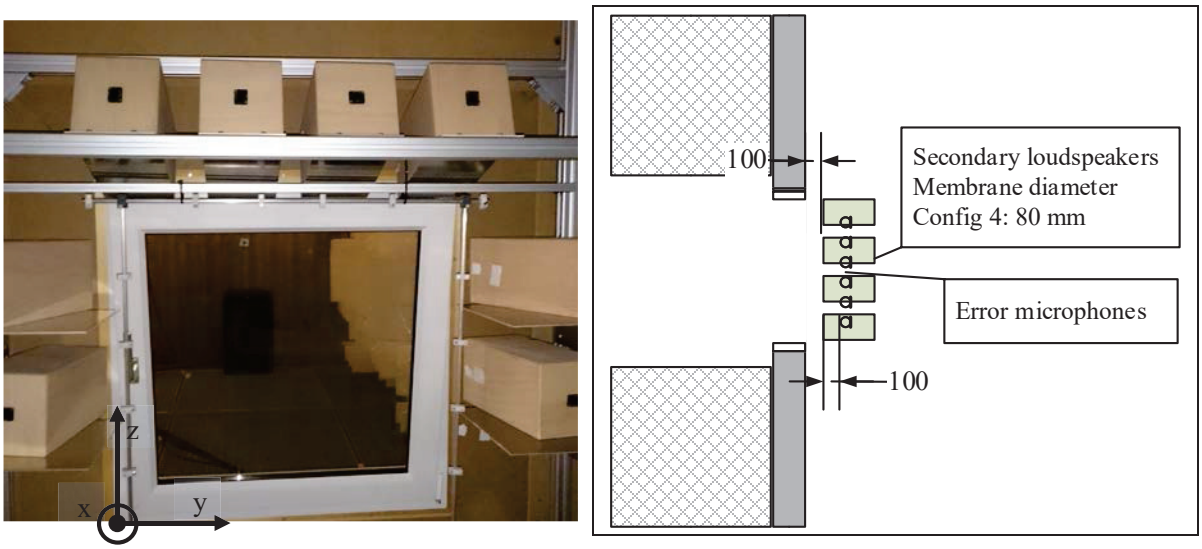

Figure 6 – Setup of configuration 4 front view (left), overview (right)

The frame [7] shown in Figure 2 (right) was meant to serve as an add-on kit to realize the ANB at an already installed window. It holds 16 secondary loudspeakers with a diameter $d = 0.06$ m and 16 error microphones, all in one line. Figure 7 shows a detailed model of the frame. To evaluate the effect of the components orientation the arrangement is rebuilt with the components used for configurations 1 to 4. The setup can be seen in Figure 8. The loudspeakers are touching the wall, this means, that the distance between the window frame and the center of the membrane is 0.08 m in positive x-direction. The error microphones are placed directly at the edge of the speaker cabinets centered above the membrane.

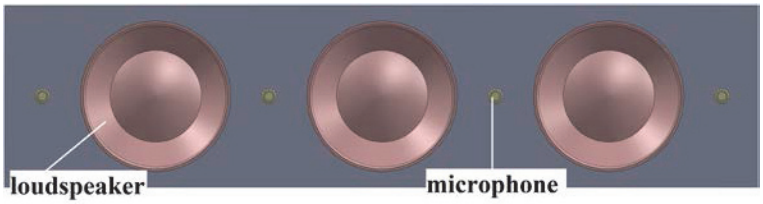

Figure 7 – Model of the ANB frame

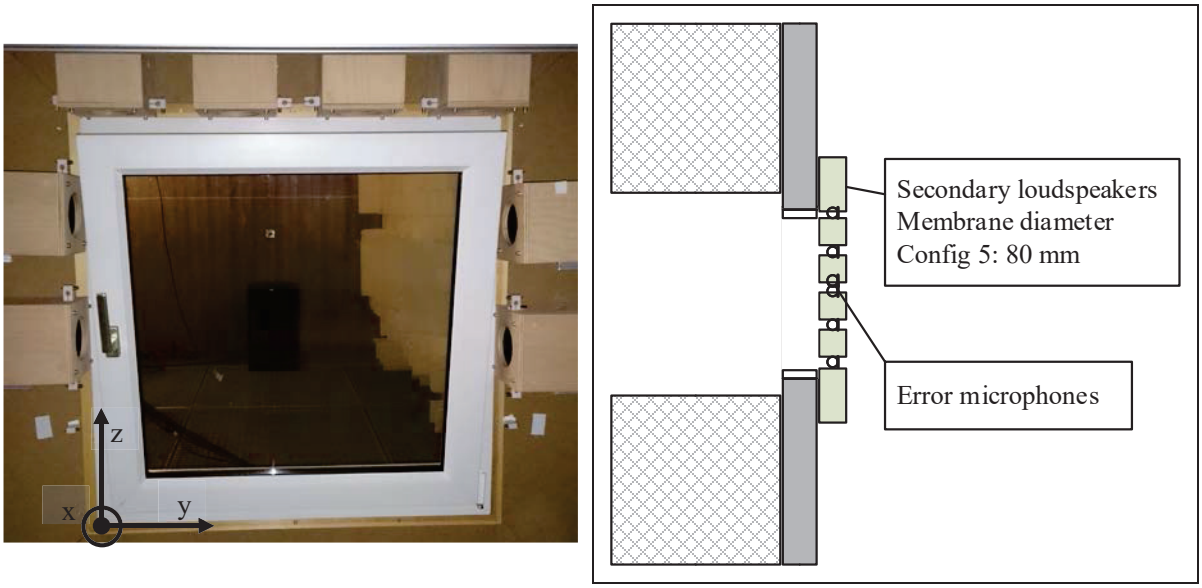

Figure 8 – Setup of configuration 5 front view (left), overview (right)

2.3 Controller

The ANB uses a feed forward FxLMS algorithm with leakage factor γ and normalized step size $\mu_n(n)$ in time domain (4). Figure 9 shows the block diagram of the system with a MIMO (multiple input multiple output) FxLMS algorithm. Small characters denote scalars, small bold characters denote vectors and capital bold characters denote matrices. The thin lines symbolize single signals, the bold lines symbolize arrays of signals. The dotted encasing marks the part of the system which is executed on the real time operating system (RTOS). This means, the reference signal is not recorded by a microphone, but it is directly handed over to the LMS after its generation.

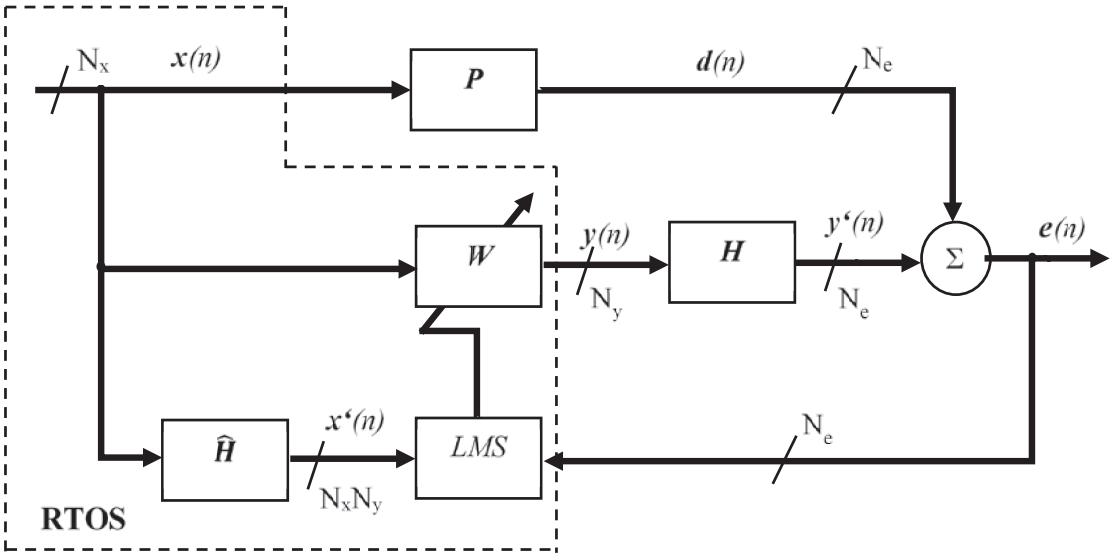

Figure 9 – Block diagram of system with filtered x LMS algorithm

At every discrete time step n the controller has to calculate $j = 1 \ldots N_y$ output signals $\boldsymbol{y}(n)$

$$y_j(n) = \sum_{i=1}^{N_x} \boldsymbol{w}_{j,i}^T(n)\boldsymbol{x}_i(n) \tag{1}$$

where $\boldsymbol{w}_{j,i}(n)$ denotes the vectors of filter coefficients of an adaptive FIR (finite impulse response) filter with $l = 1 \ldots N_w$ coefficients. $\boldsymbol{x}_i(n) = [x_i(n)\, x_i(n-1) \ldots x_i(n-N_w+1)]^T$ is the vector with the samples of the i-th reference signal. The update of the $N_x N_y$ impulse responses $\boldsymbol{w}_{i,j}$ is given by

$$\boldsymbol{w}_{i,j}(n+1) = \gamma \boldsymbol{w}_{i,j}(n) - \mu_n(n) \sum_{k=1}^{N_e} \boldsymbol{x}'_{i,j,k}(n) e_k(n) \tag{2}$$

with $k = 1 \ldots N_e$ as number of the error signals $\boldsymbol{e}(n)$ and $\boldsymbol{x}'_{i,j,k}(n)$ as N_x reference signals filtered respectively by the $N_y N_e$ internal models $\hat{\boldsymbol{H}}(z)$ of the secondary paths $\boldsymbol{H}(z)$. γ denotes the leakage factor as a weight for the past filter coefficient $w_{i,j}(n)$. The step size is normalized by

$$\mu_n(n) = \mu/\varepsilon, \text{ if } p(n) < \varepsilon \tag{3}$$

$$\mu_n(n) = \mu/p\,(n), \text{ if } p(n) \geq \varepsilon \tag{4}$$

The normalization of μ using the estimated power $p(n)$ accelerates the convergence time by increasing the step size if the power of the reference signal is low and vice versa.

$$p(n+1) = \beta p(n) + (1-\beta)x^2(n+1) \tag{5}$$

is the update of the estimated power using the smoothing factor β to weight the current value $x^2(n+1)$ the more the bigger it is defined. To prevent the step size from becoming too big it is limited by the value ε if the power is too small.

3. EXPERIMENTAL RESULTS

The measurements are executed with a broadband disturbance, using band limited white noise in the frequency range between 100 Hz and 1 kHz. The ambient noise inside the transmission test system is determined to 30 dB in the respective frequency range. The window position was tilted. The primary noise is adjusted to 74 dB at the monitoring microphone pointing towards the window. Respecting the direction of view it is the microphone on the right side of the artificial head. The amplification of the secondary sources is adapted that there is an equal level at every error microphone when using the respective secondary loudspeaker. To guarantee the comparability among the different configurations the controller parameters are fixed for all measurements as shown in table 1.

Table 1 – Controller parameters

Parameter	N_x	N_y	N_e	N_w	N_h	γ	μ	ε	β
Value	1	8	14	512	128	0.99	0.0001	0.1	0.99

Figures 10 to 14 show the results at the right monitoring microphone. The red graph shows the auto-power spectrum level of the primary noise in uncontrolled state and the blue graph the auto-power spectrum level of the resulting noise in controlled state. The control success in the frequency range from 100 Hz to 1 kHz is mentioned as $\Delta_{1...5}$ in the respective caption label.

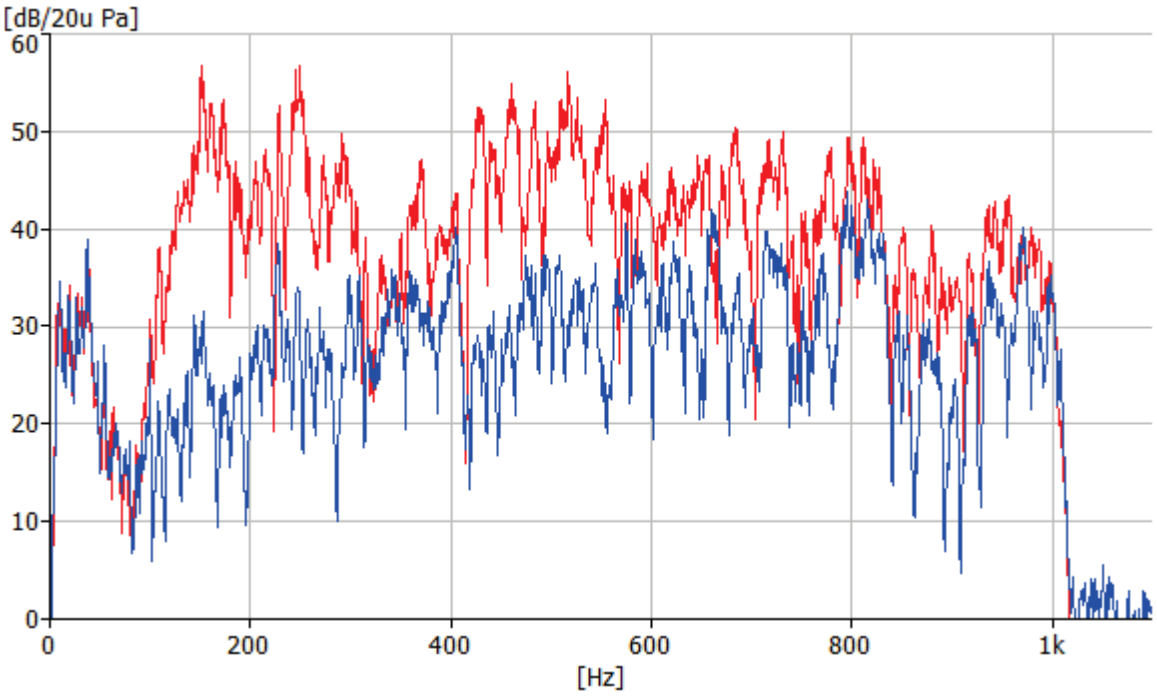

Figure 10 – Results of configuration 1 ($\Delta_1 = 12$ dB)

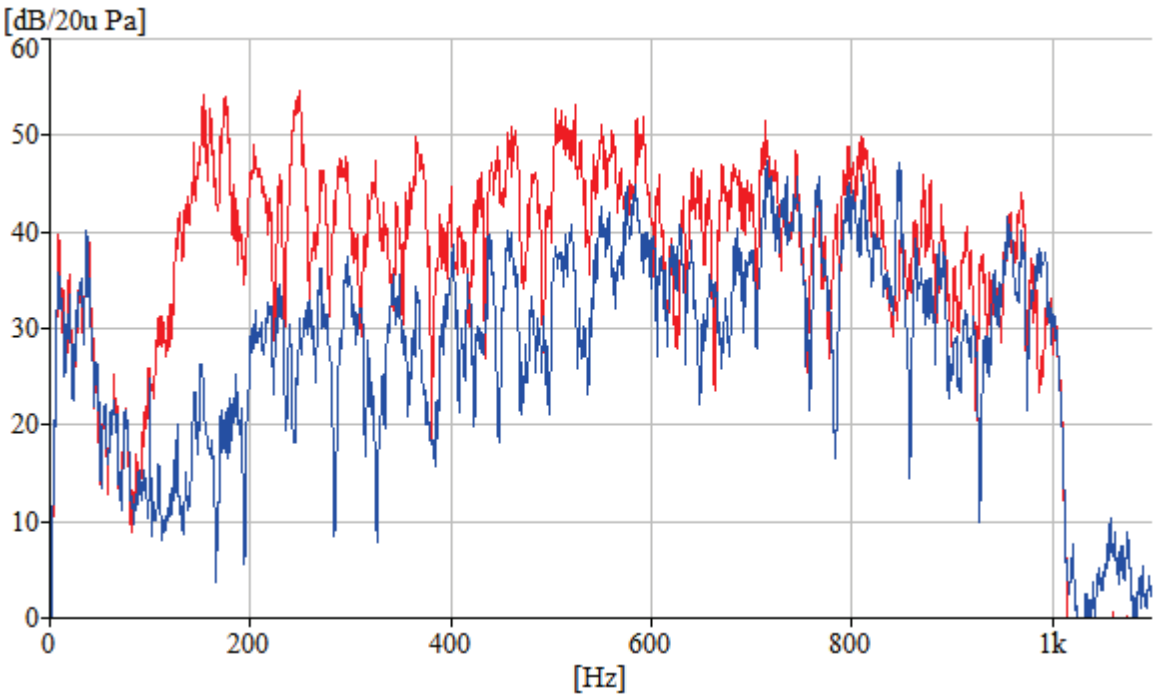

Figure 11 – Results of configuration 2 ($\Delta_2 = 9$ dB)

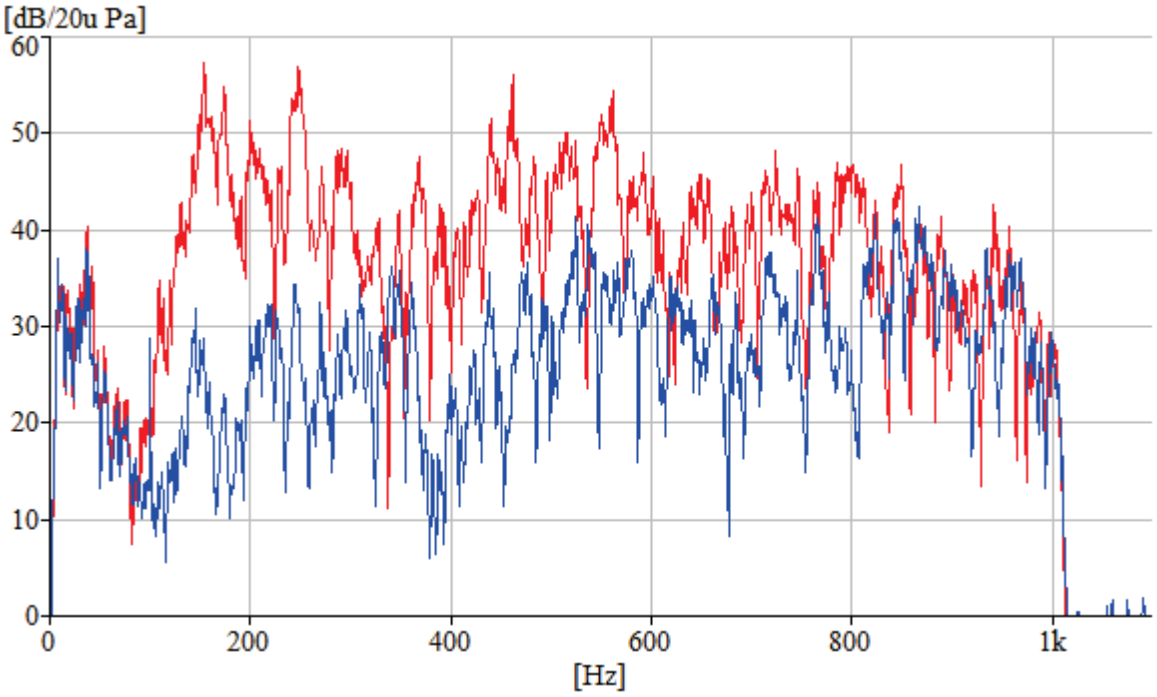

Figure 12 – Results of configuration 3 ($\Delta_3 = 13$ dB)

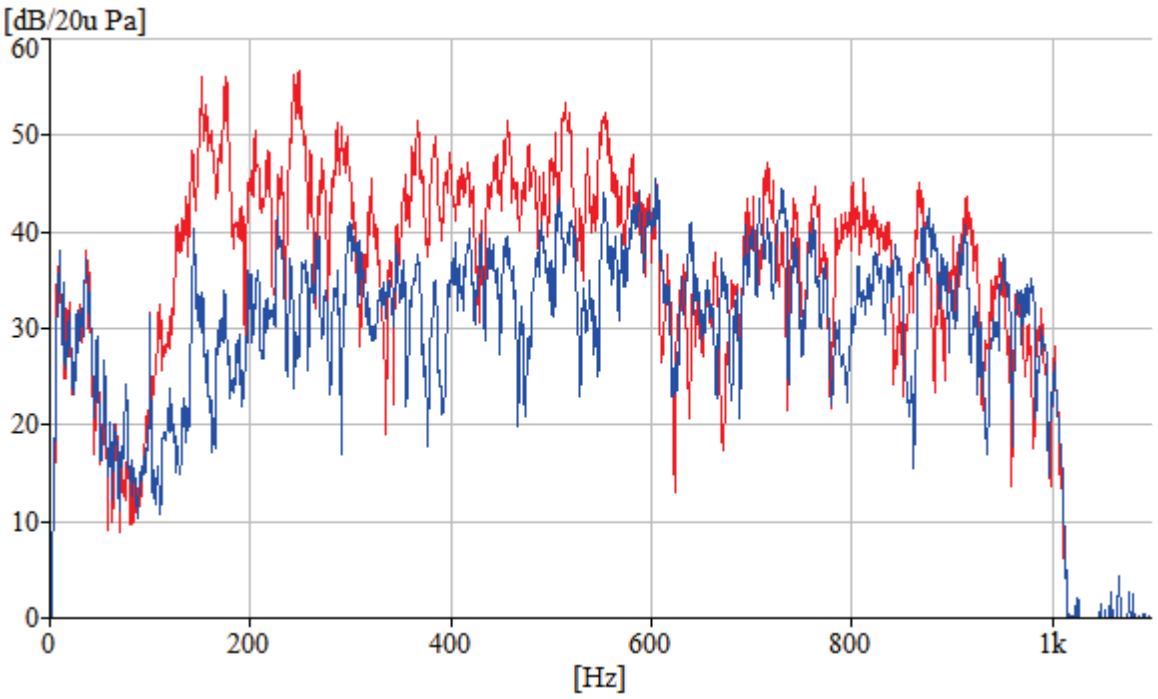

Figure 13 – Results of configuration 4 ($\Delta_4 = 8$ dB)

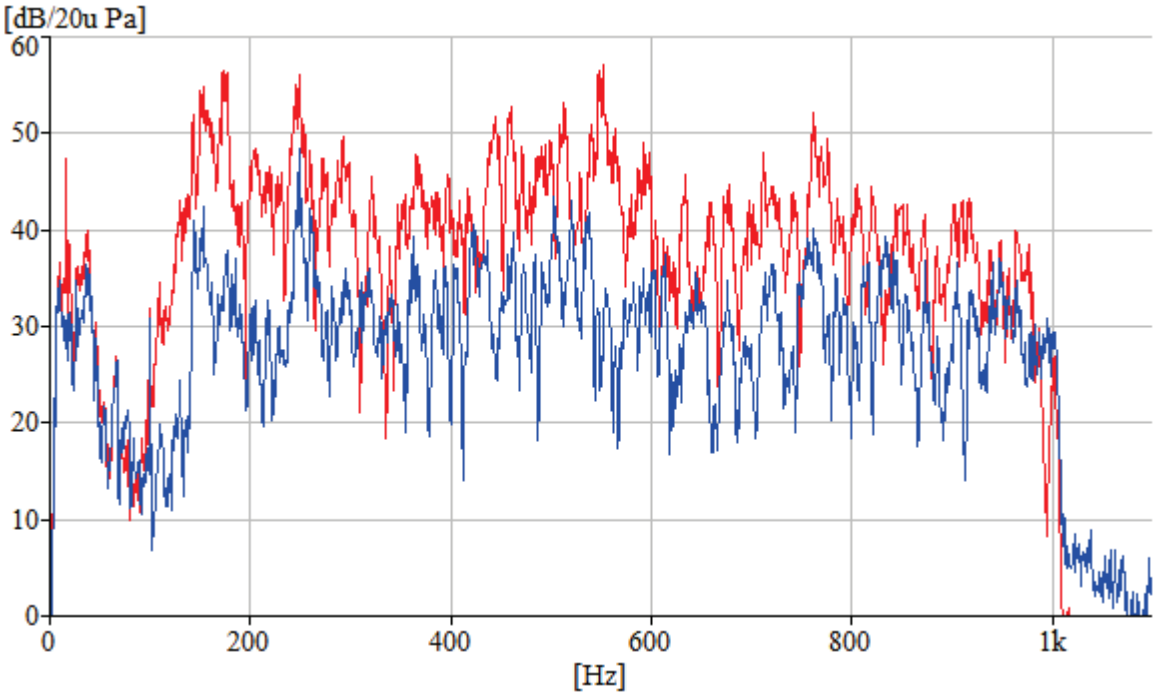

Figure 14 – Results of configuration 5 ($\Delta_5 = 12$ dB)

Comparing all 5 measurements it can be seen, that the controller achieves a higher reduction at higher primary levels. Notches in the auto-power spectrum can lead to amplification, since the controller tries to reduce the quadratic mean of the error signals. E.g. figure 12 shows, that at the frequency 342 Hz the controller amplifies the noise from 11 dB to 32 dB.

The current setup of error microphones is not sufficient to allow the controller to efficiently control higher frequencies. It can be seen that in the frequency range from 800 Hz to 1 kHz the attenuation decreases significantly compared to the frequency range from 100 Hz to 800 Hz. E.g. with

configuration 3 the attenuation between 100 Hz and 800 Hz is 15 dB whereas it is 4 dB between 800 Hz and 1 kHz. The overall result is 13 dB. A sufficient density of error microphones is crucial to sense high frequencies effectively by avoiding to place a microphone in a wave node.

Comparing the results it must be said, that all parameters were fixed. This means, that with adapting the parameters to every single setup the results could improve. This was however not the subject of this paper.

Figure 12 shows, that the smaller loudspeakers are perfectly able to achieve the same attenuation as the reference setup in configuration 1. The step from configuration 3 to 4 shows that the quality of sensing by the error microphones is crucial to the control success. Due to the relativly big loudspeaker cabinets and the short distance between the window frame and the secondary speakers the gap between the frame and the cabinets to sense the noise was very small. This disadvantage was improved with configuration 5 which yielded in an improvement of attenuation of 4 dB. It also proves, compared with configuration 3, that the orientation of the loudspeakers, if they are directed parallel or normal to the transmission path has no significant influence.

4. CONCLUSION

Different arrangements of the system components of an ANB for noise reduction in enclosed rooms are investigated. It is found that the placing of the error microphones is crucial to the control success. Obstacles near to the microphones or small gaps for sensing decrease the control success significantly. The acoustic effect of big loudspeaker cabinets which block the sound transmission path has to be considered. A high density of microphones prevents the noise from entering the cavity uncontrolled. Furthermore a possible solution for an ANB add-on kit is introduced and investigated. It is found, that the orientation of the loudspeakers has no big influence on the control success. A reduction of the loudspeakers diameter from 0.016 m to 0.008 m does not affect the control success negatively, as long as their maximal power and recommended cabinet volume is respected.

REFERENCES

1. Elliott SJ. Signal Processing for Active Control. San Diego, Calif.: Academic Press; 2001. (Signal processing and its applications).
2. Greßkowski J, Böhme S, Sachau D. Global Active Noise Control in Aircraft Cabins. In: 15th AIAA/CEAS Aeroacoustics Conference (30th AIAA Aeroacoustics Conference); 2009 .
3. Böhme S, Sachau D, Kletschkowski T. Aktive akustische Barriere. In: Fortschritte der Akustik: DAGA 2007 ; 33. Jahrestagung für Akustik, 19. bis 22. März 2007 in Stuttgart. Berlin: Dt. Ges. für Akustik; 2007. p. 695–6 .
4. Kuo SM, Morgan DR. Active noise control systems: Algorithms and DSP implementations. New York, NY: Wiley; 1996. (A Wiley-Interscience publication). Available from: URL:http://www.loc.gov/catdir/description/wiley031/95038339.html.
5. Kletschkowski T, Sachau D. Globale Lärmminderung durch lokalen Gegenschall im Transmissionspfad. In: Fortschritte der Akustik: DAGA 2012 ; 38. Deutsche Jahrestagung für Akustik ; 19. - 22. März 2012 in Darmstadt ; Tagungsband. Berlin: Deutsche Gesellschaft für Akustik; 2012. p. 753–4 .
6. Sachau D, Jukkert S. Real-time implementation of the frequency-domain FxLMS algorithm without block delay for an adaptive noise blocker. In: Proceedings of ISMA 2014. p. 93–105 .

Appendix

Tables 2 and 3 contain the coordinates of the system components for each configuration and the orientation of the perpendicular (P) on the respective speakers membrane. The origin (point (0,0,0)) of the right handed Cartesian coordinate system is defined in the lower left corner of the outer window frame. The coordinates for the loudspeakers refer to the center of the imaginary plane above the speakers membrane. All dimensions are in mm. Both, secondary loudspeakers (LS) and microphones (M) are numbered clockwise beginning in the lower left corner, looking in negative z-direction, with number 1.

Table 2 – Coordinates of centers of loudspeakers membranes

LS	1	2	3	4	5	6	7	8
Configuration 1 and 2								
x	-400	-400	-400	-400	-400	-400	-400	-400
y	125	125	125	345	565	785	785	785
z	300	520	840	840	840	840	520	300
P	(1,0,0)	(1,0,0)	(1,0,0)	(1,0,0)	(1,0,0)	(1,0,0)	(1,0,0)	(1,0,0)
Configuration 3								
x	-100	-100	-100	-100	-100	-100	-100	-100
y	125	125	125	345	565	785	785	785
z	300	520	840	840	840	840	520	300
P	(1,0,0)	(1,0,0)	(1,0,0)	(1,0,0)	(1,0,0)	(1,0,0)	(1,0,0)	(1,0,0)
Configuration 4								
x	100	100	100	100	100	100	100	100
y	125	125	125	345	565	785	785	785
z	300	520	840	840	840	840	520	300
P	(-cos20°, sin20°,0)	(-cos30°, sin30°,0)	(-cos20°, 0,-sin20°)	(-cos20°, 0,-sin20°)	(-cos20°, 0,-sin20°)	(-cos20°, 0,-sin20°)	(-cos30°, -sin30°,0)	(-cos20°, -sin20°,0)
Configuration 5								
x	80	80	80	80	80	80	80	80
y	0	0	80	335	575	830	900	900
z	460	690	900	900	900	900	690	460
P	(0,1,0)	(0,1,0)	(0,0,-1)	(0,0,-1)	(0,0,-1)	(0,0,-1)	(0,-1,0)	(0,-1,0)

Table 3 – Coordinates of centers of microphone capsules

M	1	2	3	4	5	6	7	8	9	10	11	12	13	14
Configuration 1,2 and 3														
x	100	100	100	100	100	100	100	100	100	100	100	100	100	100
y	0	0	0	0	50	210	370	530	690	850	900	900	900	900
z	300	450	600	750	900	900	900	900	900	900	750	600	450	300
Configuration 4														
x	200	200	200	200	200	200	200	200	200	200	200	200	200	200
y	50	50	50	50	0	210	370	530	690	900	850	850	850	850
z	300	450	600	750	900	900	900	900	900	900	750	600	450	300
Configuration 5														
x	80	80	80	80	80	80	80	80	80	80	80	80	80	80
y	0	0	0	0	-25	185	420	490	725	925	900	900	900	900
z	230	355	565	795	900	900	900	900	900	900	795	565	355	230